

Quantum Tricriticality and Phase Transitions in Spin-Orbit Coupled Bose-Einstein Condensates

Yun Li¹, Lev P. Pitaevskii^{1,2}, and Sandro Stringari¹

¹*Dipartimento di Fisica, Università di Trento and INO-CNR BEC Center, I-38123 Povo, Italy and*
²*Kapitza Institute for Physical Problems, Kosygina 2, 119334 Moscow, Russia*

We consider a spin-orbit coupled configuration of spin-1/2 interacting bosons with equal Rashba and Dresselhaus couplings. The phase diagram of the system at $T = 0$ is discussed with special emphasis on the role of the interaction, treated in the mean-field approximation. For a critical value of the density and of the Raman coupling we predict the occurrence of a characteristic tricritical point separating the spin mixed, the phase separated and the zero momentum states of the Bose gas. The corresponding quantum phases are investigated analyzing the momentum distribution, the longitudinal and transverse spin-polarization and the emergence of density fringes. The effect of harmonic trapping as well as the role of the breaking of spin symmetry in the interaction Hamiltonian are also discussed.

PACS numbers: 67.85.-d, 05.30.Rt, 03.75.Mn, 71.70.Ej

A large number of papers have been recently devoted to the theoretical study of artificial gauge fields in ultracold atomic gases (for a recent review see, for example, [1]). First experimental realizations of these novel configurations have been already become available [2, 3]. This field of research looks very promising from both the theoretical and experimental point of view, due to the possibility of realizing exotic configurations of non trivial topology [4], with the emergence of new quantum phases in both bosonic [5] and fermionic [6, 7] gases, and the possibility to simulate electronic phenomena of solid state physics. In the case of Bose gases a key feature of these new systems is the possibility of revealing Bose-Einstein condensation in single-particle states with nonzero momentum.

By tuning the Raman coupling between two hyperfine states of ⁸⁷Rb atoms, the authors of [3] have reported the first experimental identification of the new quantum phases exhibited by a spin-orbit coupled Bose-Einstein condensation. Important features of the resulting phases were anticipated in the paper by Ho and Zhang [8] and discussed in the same experimental paper [3]. The purpose of this Letter is to provide a theoretical description of the phase diagram corresponding to the spin-orbit coupled Hamiltonian employed in [3]. We point out the occurrence of an important density dependence in the phase diagram which shows up in the appearance of a tricritical point that, to our knowledge, has never been predicted for such systems.

We will consider the mean-field energy functional (for simplicity we set $\hbar = m = 1$)

$$E(\psi_a, \psi_b) = \int d^3r \left[(\psi_a^* \ \psi_b^*) h_0 \begin{pmatrix} \psi_a \\ \psi_b \end{pmatrix} + \frac{g_{aa}}{2} |\psi_a|^4 + \frac{g_{bb}}{2} |\psi_b|^4 + g_{ab} |\psi_a|^2 |\psi_b|^2 \right] \quad (1)$$

describing an interacting spin-1/2 Bose-Einstein condensate at $T = 0$, where ψ_a and ψ_b are the condensate wave functions relative to the two spin components interact-

ing with the coupling constants $g_{ij} = 4\pi a_{ij}$, with a_{ij} the corresponding s -wave scattering lengths, and

$$h_0 = \frac{1}{2} \left[(p_x - k_0 \sigma_z)^2 + p_\perp^2 \right] + \frac{\Omega}{2} \sigma_x + \frac{\delta}{2} \sigma_z + V_{\text{ext}} \quad (2)$$

is the single-particle Hamiltonian characterized by equal contributions of Rashba [9] and Dresselhaus [10] spin-orbit couplings and a uniform magnetic field in the $x-z$ plane. In Eq.(2) Ω is the Raman coupling constant accounting for the transition between the two spin states, k_0 is the strength associated with the spin-orbit coupling fixed by the momentum transfer of the two Raman lasers, δ fixes the energy difference between the two single-particle spin states, σ_i are the usual 2×2 Pauli matrices, while V_{ext} is the external trapping potential.

In the first part of the Letter we will consider uniform configurations, neglecting the effect of the trapping potential ($V_{\text{ext}} = 0$) and assume a spin symmetric interaction with $g_{aa} = g_{bb} \equiv g$ and $\delta = 0$. The effect of asymmetry will be discussed afterwards. The ground state condensate wave function will be determined using a variational procedure based on the following ansatz for the spinor wave function:

$$\begin{pmatrix} \psi_a \\ \psi_b \end{pmatrix} = \sqrt{\frac{N}{V}} \left[C_1 \begin{pmatrix} \cos \theta \\ -\sin \theta \end{pmatrix} e^{ik_1 x} + C_2 \begin{pmatrix} \sin \theta \\ -\cos \theta \end{pmatrix} e^{-ik_1 x} \right] \quad (3)$$

where N is the total number of atoms, V is the volume of the system. For a given value of the average density $n = N/V$, the variational parameters are then C_1 , C_2 , k_1 and θ . Their values are determined by minimizing the energy (1) with the normalization constraint $\sum_{i=a,b} \int d^3r |\psi_i|^2 = N$ (i.e., $|C_1|^2 + |C_2|^2 = 1$). Minimization with respect to θ yields the general relationship $\theta = \arccos(k_1/k_0)/2$ ($0 \leq \theta \leq \pi/4$), fixed by the single-particle Hamiltonian (2). Once the other variational parameters are determined, one can calculate key physical quantities like, for example, the momentum distribution

accounted for by the parameter k_1 , the longitudinal and transverse spin polarization of the gas

$$\langle \sigma_z \rangle = \frac{k_1}{k_0} (|C_1|^2 - |C_2|^2), \quad \langle \sigma_x \rangle = -\frac{\sqrt{k_0^2 - k_1^2}}{k_0} \quad (4)$$

and the density

$$n(x) = n \left[1 + 2|C_1 C_2| \frac{\sqrt{k_0^2 - k_1^2}}{k_0} \cos(2k_1 x + \phi) \right], \quad (5)$$

where ϕ is the relative phase between C_1 and C_2 . The ansatz (3) exactly describes the ground state of the single-particle Hamiltonian h_0 (ideal Bose gas). In this case, for $\Omega \leq 2k_0^2$, the energy, as a function of k_1 , exhibits two minima located at the values $\pm k_0 \sqrt{1 - \Omega^2/4k_0^4}$ and the ground state is degenerate, the energy being independent of the actual values of C_1 and C_2 . For $\Omega > 2k_0^2$ the two minima disappear and all the atoms condense into the zero momentum state $k_1 = 0$.

The same ansatz is well suited to discuss the role of interactions. By inserting (3) into (1), we find that the energy per particle $\varepsilon = E/N$ takes the form

$$\varepsilon = \frac{k_0^2}{2} - \frac{\Omega}{2k_0} \sqrt{k_0^2 - k_1^2} - F(\beta) \frac{k_1^2}{2k_0^2} + G_1 (1 + 2\beta) \quad (6)$$

where we have defined the dimensionless parameter $\beta = |C_1|^2|C_2|^2$ ($0 \leq \beta \leq 1/4$), and the function

$$F(\beta) = (k_0^2 - 2G_2) + 4(G_1 + 2G_2)\beta \quad (7)$$

with the interaction parameters $G_1 = n(g + g_{ab})/4$, $G_2 = n(g - g_{ab})/4$. The variational parameters to minimize the energy are then k_1 and β .

Let us first consider minimization with respect to k_1 . If $\Omega > 2F(\beta)$ the energy (6) is an increasing function of k_1 and the minimum takes place at $k_1 = 0$. If instead $\Omega < 2F(\beta)$ one finds that ε is minimized by the choice

$$k_1(\beta) = k_0 \sqrt{1 - \frac{\Omega^2}{4[F(\beta)]^2}}, \quad (8)$$

which generalizes the ideal gas result $F = k_0^2$. Equations (7) and (8) explicitly show that the momentum distribution is modified by the interactions. We find the following result for the energy per particle:

$$\varepsilon = -\frac{\Omega^2}{8F(\beta)} + G_1 + G_2 (1 - 4\beta). \quad (9)$$

The ground state of the system can be found by looking for the minimum of (9) with respect to β . One can easily prove that the second order derivative of (9) with respect to β is negative. This means that the minimum is achieved at the limiting values of β . The ground state is then compatible with the three following phases:

(I) The *spin mixed* or “*stripe*” phase with $k_1 \neq 0$, $\beta = 1/4$ and hence $\langle \sigma_z \rangle = 0$. In this phase the atoms condense in a superposition of two plane wave states with wave vector $\pm k_1$ and the density (5) exhibits fringes. This configuration is characterized by a degeneracy associated with the relative phase between the coefficients C_1 and C_2 which fixes the actual spatial position of stripes.

(II) The *separated* phase with $k_1 \neq 0$, $\beta = 0$ and hence $\langle \sigma_z \rangle \neq 0$, where the atoms condense into a single plane wave state with wave vector either k_1 ($C_2 = 0$) or $-k_1$ ($C_1 = 0$), the actual value being determined by a mechanism of spontaneous spin symmetry breaking.

(III) The *single minimum* or “*zero momentum*” phase with $k_1 = 0$ and $\langle \sigma_z \rangle = 0$ where the atoms condense in the zero momentum state. In this phase the gas is fully polarized along the x direction ($\langle \sigma_x \rangle = -1$).

We first notice that the spin mixed phase is compatible only with positive values of the interaction parameter G_2 , favoring antiferromagnetic configurations. In fact in the opposite case $G_2 < 0$, the first order derivative $\partial\varepsilon/\partial\beta$ is always positive and the ground state is always in the phase separated configuration (II) or in the zero momentum phase (III).

In the most interesting $G_2 > 0$ case, the system will be always in the phase (I) for small values of the Raman coupling constant Ω . If the condition

$$k_0^2 > 4G_2 + \frac{4G_2^2}{G_1} \quad (10)$$

is satisfied, the systems will exhibit a phase transition (I) to (II) at the frequency

$$\Omega^{(I-II)} = 2 \left[(k_0^2 + G_1) (k_0^2 - 2G_2) \frac{2G_2}{G_1 + 2G_2} \right]^{1/2}. \quad (11)$$

This generalizes the result derived in [8], which corresponds to the low density (or weak coupling) limit of (11), i.e., $G_1, G_2 \ll k_0^2$. The transition frequency in this limit approaches the density independent value

$$\Omega_{LD}^{(I-II)} = 2k_0^2 \sqrt{2\gamma/(1+2\gamma)} \quad (12)$$

where we have introduced the dimensionless interaction parameter $\gamma = G_2/G_1 = (g - g_{ab})/(g + g_{ab})$. By further increasing Ω , the system will enter the phase (III) at the frequency

$$\Omega^{(II-III)} = 2(k_0^2 - 2G_2) \quad (13)$$

This result, in the limit $G_2 \ll k_0^2$, was also discussed in [11]. If instead the condition (10) is not satisfied, the transition will occur directly from the phase (I) to (III) at the frequency

$$\Omega^{(I-III)} = 2(k_0^2 + G_1) - 2[(k_0^2 + G_1)G_1]^{1/2}. \quad (14)$$

In the strong coupling limit $G_1 \gg k_0^2$ (14) approaches the constant value k_0^2 .

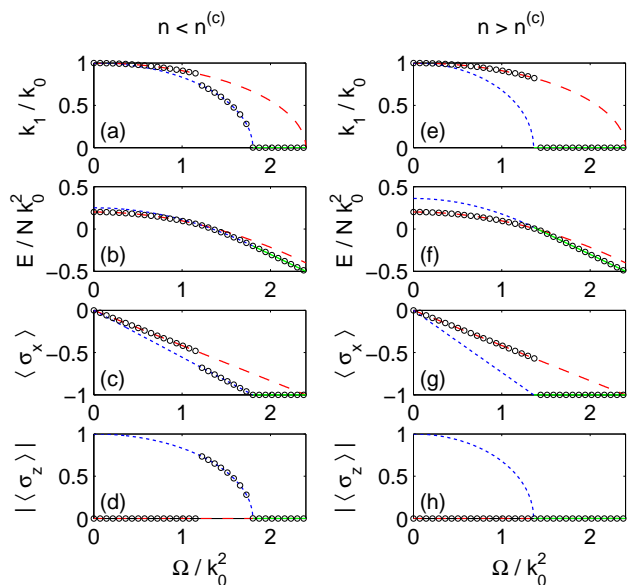


FIG. 1: (Color online) k_1 , energy per particle E/N , transverse and longitudinal spin polarization $\langle\sigma_x\rangle$ and $|\langle\sigma_z\rangle|$ as a function of Ω . Red dashed lines: stripe phase $k_1 \neq 0$ and $\beta = 1/4$; blue dotted lines: separated phase $k_1 \neq 0$ and $\beta = 0$; green solid lines: zero momentum phase $k_1 = 0$; open circles: ground state. The parameters: $G_1/k_0^2 = 0.2$, $G_2/k_0^2 = 0.05$ (a)-(d), $G_2/k_0^2 = 0.16$ (e)-(h).

The critical point where the phase (II) disappears is fixed [see Eq.(10)] by the condition $G_1^{(c)} = k_0^2/4\gamma(1+\gamma)$, corresponding to the critical value

$$n^{(c)} = k_0^2/(2\gamma g) \quad (15)$$

for the density. If $n < n^{(c)}$, one has two transitions (I-II and II-III), while if $n > n^{(c)}$, only one phase transition (I-III) can take place.

In Fig.1, we plot the momentum k_1 , the energy per particle E/N , the transverse and longitudinal spin polarizations $\langle\sigma_x\rangle$ and $|\langle\sigma_z\rangle|$ as a function of Ω for $n < n^{(c)}$ (left column) and for $n > n^{(c)}$ (right column). In addition to the results for the ground state (open circles), we also show the various quantities for the three phases (colored lines). Figures (a)-(d) reveals the emergence of the phase transitions (I-II) and (II-III), while in (e)-(h) there is only the transition (I-III). The figures also show that the transitions (I-II) and (I-III) are accompanied by a jump in k_1 [see (a) and (e)] and consequently in $\langle\sigma_x\rangle$ [see (c) and (g)]. In particular the jump in k_1 associated with the transition (I-III) is sizable and should be easily observable in experiments. On the other hand only the transition (I-II) is accompanied by a jump in the longitudinal spin polarization $|\langle\sigma_z\rangle|$. The transition (II-III) is instead characterized by a continuous behavior of the relevant physical parameters. The experimental conditions of [3] correspond to values of the average density n much smaller than $n^{(c)}$, so the jump in k_1 could not be

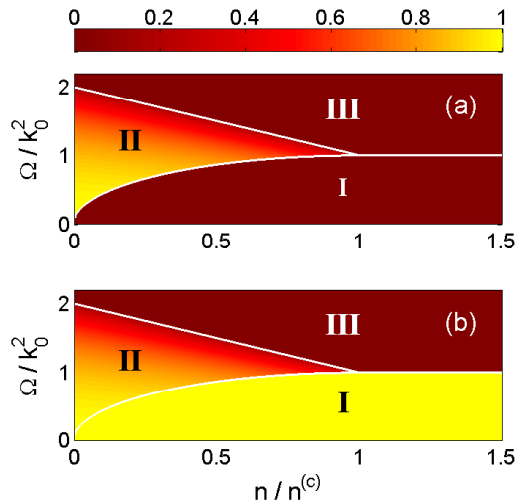


FIG. 2: (Color online) Spin polarization $|\langle\sigma_z\rangle|$ (a) and k_1/k_0 (b) as a function of Ω and density $n/n^{(c)}$ in three different phases with $G_2 > 0$. The white solid lines represent the phase transition (I-II), (II-III) and (I-III). The parameters: $g = 100 a_B$, where a_B is the Bohr radius, $\gamma = 0.0012$, $k_0^2 = 2\pi \times 80 \text{ Hz}$, corresponding to $n^{(c)} = 4.37 \times 10^{15} \text{ cm}^{-3}$.

detected because it is too small at the transition (I-II). On the other hand the occurrence of this phase transition was clearly revealed by the analysis of the spin distribution after time of flight (see Fig.2c of [3]).

In Fig.2 we show the phase diagram for the three different phases. The value of the spin polarization $|\langle\sigma_z\rangle|$ and k_1 are reported in (a) and (b) respectively. The transition lines separating different phases merge at a tricritical point at $n = n^{(c)}$. The value of $|\langle\sigma_z\rangle|$ always vanishes for $n > n^{(c)}$. However the phase transition (I-III) is well identified by the behavior of the momentum k_1 . The parameters employed in Fig.2 correspond to rather large values of the critical density. More accessible values of $n^{(c)}$ can be obtained employing smaller values of k_0 or larger values of γ using different spin states or different atomic species. Reducing the value of k_0 would also have the advantage of increasing the spatial separation between the fringes in the stripe phase (I), thereby making their experimental detection easier.

The description of the quantum phases carried out in the present work is based on the mean-field picture which ignores the role of quantum fluctuations. In ordinary Bose-Einstein condensed gases the mean-field approach is justified if the gas parameter na^3 is small. The spin-orbit term in the single-particle Hamiltonian (2) is expected to emphasize the role of quantum fluctuations. In particular when the phase (III) approaches the phase (II), quantum fluctuations are enhanced and, for large values of k_0 , the usual Bogoliubov $\sqrt{na^3}$ dependence of

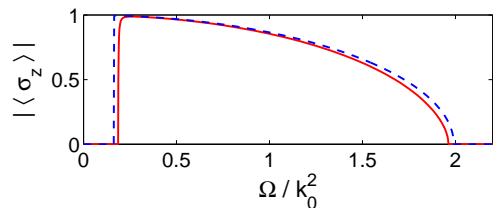


FIG. 3: (Color online) Spin polarization $|\langle\sigma_z\rangle|$ as a function of Ω for the trapped case (red solid line), and for the uniform case using the density in the center of the trap (blue dashed line). The parameters are chosen as follows: $\omega_0 = 2\pi \times 20$ Hz, $k_0^2/\omega_0 = 4$, $g_{aa} = g_{bb} = 101.20 a_B$, $g_{ab} = 100.99 a_B$, where a_B is the Bohr radius. The density in the center of trap corresponds to $n \simeq 3.9 \times 10^{13} \text{ cm}^{-3}$.

the quantum depletion of the condensate is increased by the factor $(k_0^2/gn)^{1/4}$. The effect is however small for the current values of the spin-orbit parameters.

Let us now discuss the effect of the trap. In order to simplify the analysis we have considered harmonic trapping with frequency ω_0 only along the x -axis. Without interaction, one can calculate the ground state using a similar variation ansatz, replacing the plane waves in (3) by the functions $e^{\pm ik_1 x} e^{-\omega_0 x^2/2}$, corresponding, in the absence of the gauge field, to the usual harmonic oscillator Gaussians. The energy per particle is easily calculated and reads:

$$\begin{aligned} \varepsilon = & \frac{\omega_0}{2} + \frac{k_0^2 - k_1^2}{2} - \frac{\Omega}{2k_0} \sqrt{k_0^2 - k_1^2} \\ & - (C_1^* C_2 + C_2^* C_1) \Omega \frac{k_1^2}{2k_0^2} e^{-k_1^2/\omega_0}. \end{aligned} \quad (16)$$

The ground state can be found by minimizing ε with respect to k_1 , C_1 and C_2 with the normalization constraint. The first term in (16) is just the zero point energy due to the presence of the trap. The following two terms are the same as for the uniform case without interactions, i.e., (6) with $G_1 = G_2 = 0$. The last term shows the effect of the trap, fixing the relative phase between the coefficients C_1 and C_2 in the ground state. Consequently the degeneracy occurring in the uniform case will be lifted even in the absence of interactions (where $\phi = 0$). Physically this is the consequence of the non orthogonality of the two Gaussian states. According to (16), for $k_1 \neq 0$, the system prefers to stay in the spin mixed phase, and exhibits density modulation in space even without interactions. On the other hand, the interaction is crucial for the appearance of the phase separated configuration. Since the last term of (16) scales exponentially, the effect of the trap is weak for $k_1^2 \gg \omega_0$, and becomes more and more important when k_1^2 is comparable to ω_0 .

To describe the role of the interaction we implement the mean-field approximation by solving numerically the Gross-Pitaevskii equation for the condensate wave function using the gradient method in the same 1D trapping

conditions. We find that the properties discussed in the first part of the work for the uniform system almost hold in the trapped case. In Fig.3 we show an example of the numerical calculation. The spin polarization as a function of Ω , in the presence of trapping (red solid line), is compared with our analytical results for the uniform case (blue dashed line), using the density in the center of the trap. There is good agreement between the two curves. We have checked that a similar good agreement is ensured also for larger values of the interaction parameter $n/n^{(c)}$, confirming the general validity of the ansatz (3) for the spinor wave function employed in the first part of the Letter.

We finally discuss the case $\delta \neq 0$ and $g_{aa} \neq g_{bb}$, corresponding to broken spin symmetry. In general one can introduce three interaction parameters: $G_1 = n(g_{aa} + g_{bb} + 2g_{ab})/8$, $G_2 = n(g_{aa} + g_{bb} - 2g_{ab})/8$, and $G_3 = n(g_{aa} - g_{bb})/4$. In the case of ^{87}Rb atoms, the scattering lengths relative to the spin states $|F=1, m_F=0\rangle$ and $|F=1, m_F=-1\rangle$ are usually parameterized as $a_{aa} \equiv c_0$, $a_{bb} = c_0 + c_2 = a_{ab}$, with $c_0 = 7.79 \times 10^{-12} \text{ Hz cm}^3$ and $c_2 = -3.61 \times 10^{-14} \text{ Hz cm}^3$. This corresponds to $0 < G_2 = G_3 \ll G_1$. However, since the differences among the scattering lengths are very small, by properly choosing the detuning δ , this effect can be well compensated, and the properties of the ground state remain the same as for the spin symmetric case. For example, using first order perturbation theory, one finds that correction to the energy per particle is

$$\varepsilon^{(1)} = \left(G_3 + \frac{\delta}{2} \right) \frac{k_1}{k_0} (|C_1|^2 - |C_2|^2) \quad (17)$$

where we have considered the low density (weak coupling) limit. By choosing $\delta = -2G_3$ the correction (17) identically vanishes and the transition frequencies are not consequently affected by the inclusion of the new terms in the Hamiltonian. Using the ^{87}Rb parameters introduced above we find the value $\Omega_{\text{LD}}^{(I-II)} = 0.19 E_L$ ($E_L = k_0^2/2$) in agreement with the findings of [3] corresponding to $n/n^{(c)} \ll 1$. For higher densities, the value of δ should depend on Ω dependent in order to ensure exact compensation.

In conclusion, we have investigated the phase diagram of spin-orbit coupled two-component Bose-Einstein condensates using a variation ansatz based on the mean-field approximation. We predict a rich phase diagram characterized by the occurrence of three different quantum phases, and by a characteristic tricritical point where the three phases merge at a critical value of the density and of the Raman frequency. Important questions that remain to be investigated are the dynamic properties of the system and its behavior at a finite temperature.

Useful discussions with I. Spielman and H. Zhai are acknowledged. This work has been supported by ERC through the QGBE grant and by the Italian MIUR through the PRIN-2009 grant.

-
- [1] J. Dalibard, F. Gerbier, G. Juzeliūnas, and P. Öhberg, *Rev. Mod. Phys.* **83**, 1523 (2011).
- [2] Y.-J. Lin, R. L. Compton, K. Jiménez-García, J. V. Porto, and I. B. Spielman, *Nature*, **462**, 628 (2009); Y.-J. Lin, R. L. Compton, K. Jiménez-García, W. D. Phillips, J. V. Porto, and I. B. Spielman, *Nature Phys.* **7**, 531 (2011).
- [3] Y.-J. Lin, K. Jiménez-García, and I. B. Spielman, *Nature*, **471**, 83 (2011).
- [4] M. Z. Hasan and C. L. Kane, *Rev. Mod. Phys.*, **82**, 3045 (2010).
- [5] T. D. Stanescu, B. Anderson, and V. Galitski, *Phys. Rev. A*, **78**, 023616 (2008); C. Wang, C. Gao, C.-M. Jian, and H. Zhai, *Phys. Rev. Lett.*, **105**, 160403 (2010); C.-J. Wu, I. Mondragon-Shem and X.-F. Zhou, *Chin. Phys. Lett.*, **28**, 097102 (2011).
- [6] J. P. Vyasankere and V. B. Shenoy, *Phys. Rev. B*, **83**, 094515 (2011); J. P. Vyasankere, S. Zhang, and V. B. Shenoy, *Phys. Rev. B*, **84**, 014512 (2011).
- [7] M. Gong, S. Tewari, and C. Zhang, *Phys. Rev. Lett.*, **107** 195303 (2011); H. Hu, L. Jiang, X.-J. Liu, and H. Pu, *Phys. Rev. Lett.*, **107**, 195304 (2011); Z.-Q. Yu and H. Zhai, *Phys. Rev. Lett.*, **107**, 195305 (2011).
- [8] T.-L. Ho and S. Zhang, *Phys. Rev. Lett.*, **107**, 150403 (2011).
- [9] Y. A. Bychkov and E. I. Rashba, *J. Phys. C*, **17**, 6039 (1984).
- [10] G. Dresselhaus, *Phys. Rev.*, **100**, 580 (1955).
- [11] Y. Zhang, G. Chen, and C. Zhang, arXiv:1111.4778.